

## RESEARCH ARTICLE

# Accelerated Adaptive Gradient Neural Dynamics Models for Solving Time-Variant Lyapunov Equation and Their Applications

QINROU LI<sup>1</sup>, YUYUAN ZHUANG<sup>2</sup>, LILAN ZOU<sup>1</sup>, AND GUANCHENG WANG<sup>1</sup><sup>1</sup>College of Electronic and Information Engineering, Guangdong Ocean University, Zhanjiang 524088, China<sup>2</sup>College of Mathematics and Computer Science, Guangdong Ocean University, Zhanjiang 524088, China

Corresponding authors: Guancheng Wang (wanggc@gdou.edu.cn) and Lilan Zou (zoulilan2015@163.com)


This work was supported in part by the National Natural Science Foundation of China under Grant 62272109, in part by the Guangdong University Student Science and Technology Innovation Cultivation Special Fund Support Project under Grant pdjh2023 a0243, in part by the Undergraduate Innovation Team Project of Guangdong Ocean University under Grant CXTD2021019, and in part by the Undergraduate Training Program for Innovation and Entrepreneurship Training Project of Guangdong Ocean University under Grant CXXL2022158.

**ABSTRACT** The time-variant Lyapunov equation (TVLE) has played an important role in many fields due to its ubiquity and many neural dynamics models have been developed to obtain the online solution of the TVLE. In prevalent methods, the gradient neural dynamics (GND) models suffer from the large residual error due to the lack of predictive computing, while the zero neural dynamics (ZND) models have large computing complexity because of the inverse of the mass matrix in models. To mitigate these deficiencies, an adaptive parameter containing the time-derivative of time-variant parameters in the TVLE is added to the GND model to form the adaptive GND (AGND) model, which enables the AGND model predictive computing as ZND models and inherits the free of matrix inverse from the GND models. Moreover, two strategies are proposed to design the accelerated AGND (AAGND) models that enjoy a faster convergence rate. The accuracy and the convergence rate of AAGND models are theoretically analyzed, indicating that AAGND models achieve zero residual error and a faster convergence rate. In addition, numerical simulations and two applications are provided to verify the theoretical analyses and the efficiency of AAGND models. The experimental results demonstrate that the AAGND model can solve the TVLE with high accuracy and have great potentialities in applications.

**INDEX TERMS** Neural dynamics, time-variant Lyapunov equation, convergence, adaptive parameter, robotic control.

## I. INTRODUCTION

Since the Lyapunov equation was proposed, it has attracted much attention from numerous scholars due to its ubiquity in image processing [1], optimization [2], and stability analysis [3]. Moreover, the Lyapunov equation is widely used in many fields of adaptive control [4], filter design [5], and neural networks [6]. In the past few decades, many different approaches have been developed for solving and applying the Lyapunov equation. For example, Win et al. proposed a novel geometric algorithm based on the fiber bundle to solve

The associate editor coordinating the review of this manuscript and approving it for publication was Diego Oliva .

the statics Lyapunov equation, in which the experimental results demonstrated that it can have a faster convergence speed compared with other algorithms [7]. Furthermore, based on the control theory, an integration-enhanced Newton algorithm was designed as a proportional-integral feedback control system, which is superior in accuracy and robustness when solving time-variant Lyapunov equation (TVLE) [8]. However, traditional numerical methods are usually used to solve time-invariant problems. When using them to deal with time-variant problems, the accuracy of these algorithms is low due to the lack of predictive calculation [9], [10], [11].

For sake of improving the accuracy of the solution, various neural dynamics models are developed to solve the TVLE.

**TABLE 1. Comparison among various models for solving time-variant problems.**

	Model in [8]	Model in [17]	Model in [10]	Model in [12]	Model in [21]	Model in [22]	This work
Adaptive parameter	✗	✗	✓	✓	✗	✗	✓
Elimination of matrix inversion	✗	✓	✗	✗	✗	✗	✓
Zero theoretical error	✗	✗	✓	✓	✓	✓	✓

In the last decades, the zeroing neural dynamics (ZND) model originated from the Hopfield neural network has been widely investigated and applied [12], [13], [14]. It is endowed with predictive computing due to the utilization of the time derivative of time-variant parameters, which can effectively solve various time-variant problems with zero theoretical analyses. For example, from a control-theoretic point of view, a novel ZND model is proposed by Sun et al. for solving time-variant zero-finding problems, which can tolerate and suppress noises [15]. Besides this, regarding the complex-valued TVLE, a ZND model with predefined-time convergence was proposed by utilizing a particular activation function [16]. Furthermore, Jiang et al. utilized an adaptive control strategy to design the ZND model for solving time-variant matrix square root. Though the efficiency and feasibility of ZND models have been proven, limitations may occur due to involving an inversion of the mass matrix existing in ZND models. On the one hand, it requires the time-variant mass matrix always be invertible. On the other hand, the calculation of matrix inversion would significantly increase the computing workload.

As the model is widely used to solve equations, gradient neural dynamics (GND) models also have attracted much attention [17], [18], [19]. For example, a linear GND model was designed to solve the periodic Sylvester equation with a superior convergence effect [20]. In addition, Xiao et al. utilized the conventional gradient neural dynamics (CGND) model to solve time-variant linear inequality [17]. Compared with ZND models, the CGND model eliminates the inversion of the mass matrix, while it suffers from low accuracy when solving time-variant problems. To improve the accuracy of the GND model, a hybrid GND-ZND model was presented to solve time-variant matrix inversion in [21], whose solution can converge to the theoretical solution. However, it also suffers from the inversion of the mass matrix because it contains the ZND model. Moreover, a gradient-feedback ZND model, which also is a variant of the CGND model, was proposed to solve time-variant optimization with superior performance [22].

In this paper, taking the advantage of eliminating the matrix inversion in the CGND model and the predictive computing of ZND models, a novel accelerated adaptive GND (AAGND) model is proposed for solving the TVLE, which utilizes an adaptive parameter that contains the time derivative of time-variant parameters. Employing the adaptive parameter, the AAGND model acquires the property of predictive computing as well as zero theoretical error. Besides this, the AAGND retains the elimination of matrix inversion as the CGND model. Furthermore, for the sake of

accelerating the convergence rate, two strategies are proposed and employed in the AAGND model. Both the zero theoretical error and the accelerated convergence rate are proven and verified by theoretical analyses and numerical simulation. Meanwhile, two applications of the AAGND model are also demonstrated in this paper.

The rest of this paper is structured as follows. Section II introduces the form of the TVLE and the model of the traditional GND and ZND models. After that, Section III proposes the AAGND model and performs theoretical analyses regarding its superiorities. In addition, the results of numerical simulation and application are presented in Section IV. Finally, Section V concludes this paper. The main contributions of this paper are as below.

- (1) Novel AAGND models are proposed to solve the TVLE, which have advantages in the elimination of matrix inversion and predictive computing.
- (2) Two strategies are provided to accelerate the convergence of the proposed model.
- (3) The efficiency of the AAGND model is demonstrated with theoretical analyses, numerical simulations, and applications.

## II. FORMULATION OF THE PROBLEM AND RELATED WORKS

### A. PROBLEM STATEMENT

Generally, the TVLE can be depicted as

$$A^T(t)X(t) + X(t)A(t) + S(t) = 0, \quad (1)$$

where  $A(t) \in \mathbb{R}^{n \times n}$  is a time-variant smooth coefficient matrix and  $S(t) \in \mathbb{R}^{n \times n}$  is a time-variant symmetric positive-definite coefficient matrix. In addition,  $X(t) \in \mathbb{R}^{n \times n}$  is the time-variant solution of the TVLE to be solved [23], [24].

### B. CONVENTIONAL SOLVING MODELS

#### 1) THE ZEROING NEURAL DYNAMICS MODEL

The ZND model is a class of neural networks dedicated to finding zeros of equations and solving time-variant problems, which has the characteristics of zero residual error [25]. The core of the ZND is to construct an error function and track the time-variant solution by using the time derivative of the time-variant parameter [26]. The steps to build the ZND model are as below.

Defining an error function as

$$E(t) = A^T(t)X(t) + X(t)A(t) + S(t). \quad (2)$$

Then, vectorizing both sides of (2) can get

$$e(t) = N(t)x(t) + s(t), \quad (3)$$

where  $\mathbf{e}(t) \in \mathbb{R}^{n \times n}$ ,  $\mathbf{x}(t) \in \mathbb{R}^{n \times n}$ , and  $\mathbf{s}(t) \in \mathbb{R}^{n \times n}$  are the vectorization of  $E(t)$ ,  $X(t)$ , and  $S(t)$ , respectively. In addition,  $N(t) = I \otimes A^T(t) + A^T(t) \otimes I \in \mathbb{R}^{n^2 \times n^2}$ , where  $I$  is the identity matrix and  $\otimes$  denotes the Kronecker product. According to (3), the derivative of  $\mathbf{e}(t)$  can be expressed as

$$\dot{\mathbf{e}}(t) = \dot{N}(t)\mathbf{x}(t) + N(t)\dot{\mathbf{x}}(t) + \dot{\mathbf{s}}(t). \quad (4)$$

Based on the conception of the ZND model, an ordinary differential equation is defined as

$$\dot{\mathbf{e}}(t) = -\gamma \Theta(\mathbf{e}(t)), \quad (5)$$

where  $\gamma$  is a positive number affecting the convergence speed of the ZND model. The bigger the  $\gamma$  is, the faster convergence speed the ZND model has. Besides this,  $\Theta(\cdot)$  is the activation function. Inserting (4) into (5) can obtain

$$\dot{\mathbf{x}}(t) = N^{-1}(t)(-\dot{N}(t)\mathbf{x}(t) - \dot{\mathbf{s}}(t) - \gamma \Theta(\mathbf{e}(t))). \quad (6)$$

In the conventional ZND (CZND) model,  $\Theta(\cdot)$  is a linear equation. It is notable that constructing (6) involves the inversion of a matrix that requires much more floating-point operations compared with other arithmetic operations like multiplication and addition among matrices and vectors [27]. To find out the solution  $\mathbf{x}(t) \in \mathbb{R}^{n^2}$ , the ZND model consumes  $O((n^2)^3)$  floating-point operations at each time instant.

## 2) THE GRADIENT NEURAL DYNAMICS MODEL

The GND model defines a non-negative energy function in scalar norm values and then updates the solution along the negative gradient until the minimum value is found. The steps of constructing the GND model are as follows.

Set an energy function that is based on the scalar value 2-norm as

$$\boldsymbol{\varepsilon}(t) = \frac{1}{2} \|\mathbf{e}(t)\|_2^2 = \frac{1}{2} \mathbf{e}^T(t)\mathbf{e}(t) \in \mathbb{R}, \quad (7)$$

where  $\|\cdot\|_2$  represents the 2-norm of the matrix. When  $\boldsymbol{\varepsilon}(t) = 0$ , the corresponding  $\mathbf{x}(t)$  is the required theoretical solution. To get the theoretical solution, the GND model estimates the solution as

$$\dot{\mathbf{x}}(t) = -\lambda \frac{\partial \boldsymbol{\varepsilon}(t)}{\partial \mathbf{x}(t)} \mathbf{e}(t) = -\lambda N^T(t)\mathbf{e}(t). \quad (8)$$

where  $\lambda > 0$  is designed to adjust the convergence rate and accuracy of (8). Compared with the ZND model, the GND model calculates the transpose of  $N(t)$  rather than its inversion, which effectively reduces the computing complexity. To construct (8), it requires  $O((n^2)^2)$  floating-point operations.

## III. THE NOVEL AAGND MODEL

In this section, inheriting the advantages of the GND model, an adaptive GND (AGND) model is proposed by replacing the parameter  $\lambda$  in (8) with an adaptive parameter  $\sigma(t)$ . Therefore, the AGND model can be expressed as

$$\dot{\mathbf{x}}(t) = -\sigma(t)N^T(t)\mathbf{e}(t), \quad (9)$$

where

$$\sigma(t) = \alpha \frac{|\mathbf{e}^T(t)(\dot{N}(t)\mathbf{x}(t) + \dot{\mathbf{s}}(t))|}{\|\mathbf{e}^T(t)N(t)\|_2^2}. \quad (10)$$

Besides this,  $\alpha > 1$  is designed to adjust the convergence rate of (9). The AGND model (9) has additional computing of  $\sigma(t)$ , which also requires  $O((n^2)^2)$  floating-point operations. Therefore, the AGND model (9) requires more but the same level computing complexity compared with the GND model (8), while has a lower complexity than the ZND model (6). Regarding the global convergence of the AGND model (9), the following theorem is provided.

*Theorem 1:* When solving the TVLE (1) with the AGND model (9), the solution globally converges to the theoretical solution.

*Proof:* A Lyapunov candidate is defined as

$$L(t) = \frac{1}{2} \|\mathbf{e}(t)\|_2^2 = \frac{1}{2} \mathbf{e}^T(t)\mathbf{e}(t) \geq 0, \quad (11)$$

where  $L(t) = 0$  if and only if  $\mathbf{e}(t) = 0$ . Thus,  $L(t)$  is positive definite. Furthermore, its time derivative  $\dot{L}(t)$  is

$$\dot{L}(t) = \mathbf{e}^T(t)\dot{\mathbf{e}}(t) = \mathbf{e}^T(t)(N(t)\dot{\mathbf{x}}(t) + \dot{N}(t)\mathbf{x}(t) + \dot{\mathbf{s}}(t)). \quad (12)$$

Inserting (9) into (12) can get

$$\begin{aligned} \dot{L}(t) &= \mathbf{e}^T(t)(-\sigma(t)N(t)N^T(t)\mathbf{e}(t) + \dot{N}(t)\mathbf{x}(t) + \dot{\mathbf{s}}(t)) \\ &= -\sigma(t)\|\mathbf{e}^T(t)N(t)\|_2^2 + \mathbf{e}^T(t)(\dot{N}(t)\mathbf{x}(t) + \dot{\mathbf{s}}(t)) \\ &= -\alpha|\mathbf{e}^T(t)(\dot{N}(t)\mathbf{x}(t) + \dot{\mathbf{s}}(t))| + \mathbf{e}^T(t)(\dot{N}(t)\mathbf{x}(t) \\ &\quad + \dot{\mathbf{s}}(t)). \end{aligned} \quad (13)$$

Since  $\alpha > 1$ , thus  $\dot{L}(t) \leq 0$ , indicating it is negative definite. According to the Lyapunov stability theorem [28], the solution synthesized by the AGND model (9) globally converges to the theoretical one. The proof is thus complete.

With the purpose of accelerating the convergence speed of the AGND model, two strategies are proposed to construct the AAGND model. The first AAGND (AAGND-1) model can be expressed as

$$\dot{\mathbf{x}}(t) = -\exp(\|\mathbf{e}(t)\|_2)\sigma(t)N^T(t)\mathbf{e}(t). \quad (14)$$

Furthermore, in view of previous studies of ZND models, activation functions are utilized to improve the convergence rate. Therefore, the activation function is employed to construct the second AAGND (AAGND-2) model as

$$\dot{\mathbf{x}}(t) = -\sigma(t)N^T(t)\Gamma(\mathbf{e}(t)), \quad (15)$$

where  $\Gamma(\cdot)$  denotes the activation function. Compared the original AGND model (9) with the AAGND-2 model (15), the AGND model (9) is a special case of the AAGND-2 model (15) with a linear activation equation expressed as  $\Gamma(\mathbf{e}_i(t)) = \mathbf{e}_i(t)$ . In addition, the hyperbolic sine activation functions are employed to accelerate the convergence rate. An example is formulated as

$$\Gamma(\mathbf{e}_i(t)) = \frac{\exp(2\mathbf{e}_i(t))}{3} - \frac{\exp(-2\mathbf{e}_i(t))}{3}. \quad (16)$$

Regarding the convergence of the proposed AAGND-1 models (14), the following theorems have been provided.

*Theorem 2:* When solving the TVLE (1) with the AAGND-1 model (14), the obtained solution globally converges to its theoretical value with a faster convergence rate compared with the AGND model (9).

*Proof:* Defining a positive definite Lyapunov candidate  $L_1(t) = \mathbf{e}^T(t)\dot{\mathbf{e}}(t)$ , its time derivative can be expressed as

$$\begin{aligned}\dot{L}_1(t) &= \mathbf{e}^T(t)(-\exp(\|\mathbf{e}(t)\|_2)\sigma(t)N(t)N^T(t)\mathbf{e}(t) \\ &\quad + \dot{N}(t)\mathbf{x}(t) + \dot{\mathbf{s}}(t)) \\ &= -\alpha\exp(\|\mathbf{e}(t)\|_2)|\mathbf{e}^T(t)(\dot{N}(t)\mathbf{x}(t) + \dot{\mathbf{s}}(t)| \\ &\quad + \mathbf{e}^T(t)(\dot{N}(t)\mathbf{x}(t) + \dot{\mathbf{s}}(t))).\end{aligned}\quad (17)$$

Since  $\exp(\|\mathbf{e}(t)\|_2) \geq 1$  when  $t \geq 0$  and  $\alpha > 1$ ,  $\dot{L}_1(t) \leq 0$  in the AAGND-1 model (14). According to the Lyapunov stability theorem, the solution estimated by the AAGND-1 model (14) globally converges to the theoretical one. In addition, since  $\alpha\exp(\|\mathbf{e}(t)\|_2) > \alpha$  when  $t \geq 0$ ,  $|\dot{L}_1(t)|$  in the AAGND-1 model (14) is larger than  $|\dot{L}(t)|$  in the AGND model (9), indicating that the AAGND-1 model (14) has a faster convergence rate compared with the AGND model (9). The proof is thus complete.

Regarding the AAGND-2 model (15), its convergence is discussed as the following theorem.

*Theorem 3:* When solving the TVLE (1) with the AAGND-2 model (15), the obtained solution globally converges to its theoretical value with a faster convergence rate compared with the AGND model (9).

*Proof:* Defining a positive definite Lyapunov candidate as  $L_2(t) = \mathbf{e}^T(t)\dot{\mathbf{e}}(t)$ , its time derivative can be expressed as

$$\begin{aligned}\dot{L}_2(t) &= \mathbf{e}^T(t)(-\sigma(t)N(t)N^T(t)\Gamma(\mathbf{e}(t)) + \dot{N}(t)\mathbf{x}(t) + \dot{\mathbf{s}}(t)) \\ &= -\sigma(t)\mathbf{e}^T(t)N(t)N^T(t)\Gamma(\mathbf{e}(t)) + Q(t),\end{aligned}\quad (18)$$

where  $Q(t) = \mathbf{e}^T(t)\dot{N}(t)\mathbf{x}(t) + \mathbf{e}^T(t)\dot{\mathbf{s}}(t)$ . According to the proof in Theorem 1,  $\dot{L}(t) = -\sigma(t)\mathbf{e}^T(t)N(t)N^T(t)\mathbf{e}(t) + Q(t) < 0$ . Based on the definition of the activation function (16), we have  $|\Gamma(\mathbf{e}(t))| \geq \mathbf{e}(t)$ . Thus,  $\dot{L}_2(t) < \dot{L}(t) < 0$ .

Therefore, the AAGND-2 model (15) can solve the TVLE (1) with zero residual error and has a faster convergence rate compared with the AGND model (9). The proof is thus complete.

#### IV. EXPERIMENTAL RESULTS

In previous sections, AAGND models and their convergence have been investigated. To demonstrate their efficiency, numerical simulations solving a TVLE (1) are performed. Furthermore, AAGND models are exploited in two applications to demonstrate their feasibility. All the experiments are performed in MATLAB 2019b on a desktop computer with a Core i7-4770 @3.40 GHz CPU, 16 GB memory, and Microsoft Windows 10.

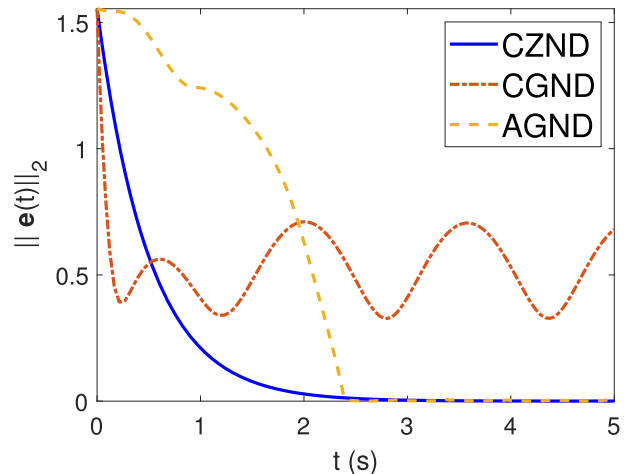


FIGURE 1. The profiles of residual errors synthesized by various models.

#### A. NUMERICAL SIMULATIONS

Considering an example of a TVLE with parameter matrices as

$$\begin{aligned}A(t) &= \begin{bmatrix} -1 - 0.5 \cos(2t) & 0.5 \sin(2t) \\ 0.5 \sin(2t) & -1 + 0.5 \cos(2t) \end{bmatrix} \in \mathbb{R}^{2 \times 2}, \\ S(t) &= \begin{bmatrix} \sin(2t) & \cos(2t) \\ -\cos(2t) & \sin(2t) \end{bmatrix} \in \mathbb{R}^{2 \times 2},\end{aligned}\quad (19)$$

various models are exploited to solve it. In the beginning, the comparison simulation among the CZND model (6), CGND model (7), and AGND model (9) is performed. With  $\gamma = \lambda = \alpha = 2$ , the trajectories of residual errors synthesized by these models are plotted in Fig. 1. As shown in Fig. 1, the CGND model (1) has much larger steady residual error compared with the CZND (6) and AGND (9) model. The steady-state residual error of the AGND (9) model converges to zero, demonstrating its property of zero theoretical error discussed in Theorem 1.

With the same  $\alpha$ , the simulations solving the TVLE (19) are performed. Fig. 2 depicts the results obtained by the AGND model (9) from five random initial states  $\mathbf{x}(0)$ , where Fig. 2(a) illustrates the trajectories of solutions and Fig. 2(b) shows the trajectories of residual errors. In Fig. 2(a), the computing solutions (blue-solid curves) can precisely track the theoretical solution (red-dotted curve). Regarding the residual errors, they can be steady and converge to zero. Specifically, as indicated in Fig. 2(b), the convergence times range from 1.66 s to 2.60 s. The same simulations with the AAGND-1 (14) and AAGND-2 (15) models are performed and results are demonstrated in Fig. 3 and Fig. 4, respectively. As shown in Fig. 3 and 4, both models can effectively solve the TVLE (19) with negligible steady residual error. Moreover, compared with the AGND model (9), the AAGND-1 (14) and AAGND-2 (15) models require less convergence time. In other words, these two models enjoy a faster convergence rate, verifying the

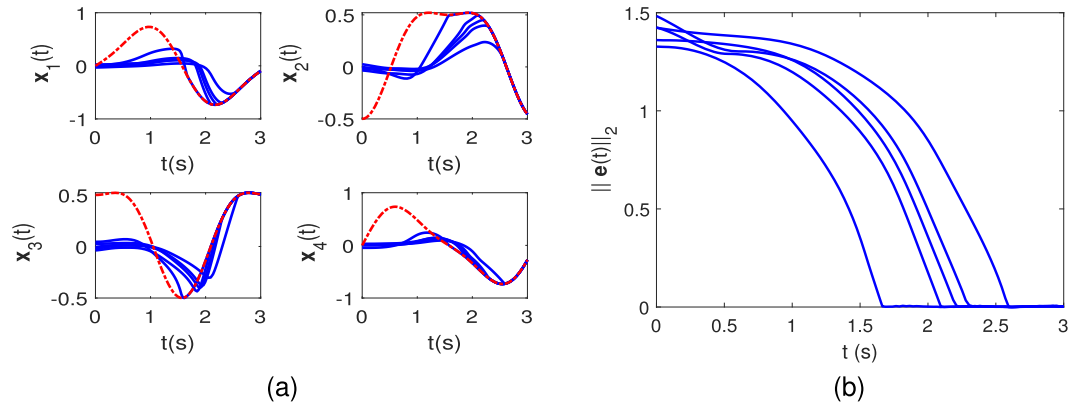


**FIGURE 2.** Simulative results of solving the TVLE problem (19) by the AGND model (9) with five random initial states. (a) The trajectories of elements of solution  $x(t)$ , where the blue-solid curves denote the computing solution and the red-dotted curve denotes the theoretical solution. (b) The trajectories of residual error  $\|e(t)\|_2$ .

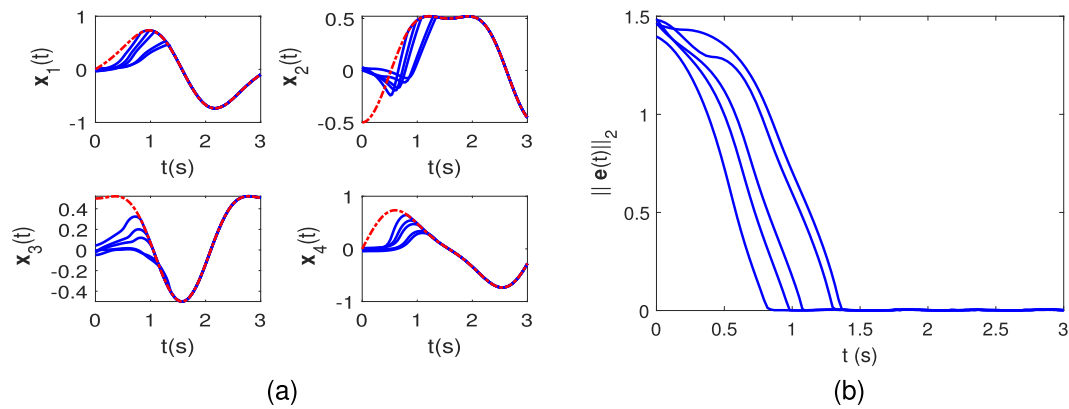


**FIGURE 3.** Simulative results of solving the TVLE problem (19) by the AAGND-1 model (14) with five random initial states. (a) The trajectories of elements of solution  $x(t)$ , where the blue-solid curves denote the computing solution and the red-dotted curve denotes the theoretical solution. (b) The trajectories of residual error  $\|e(t)\|_2$ .

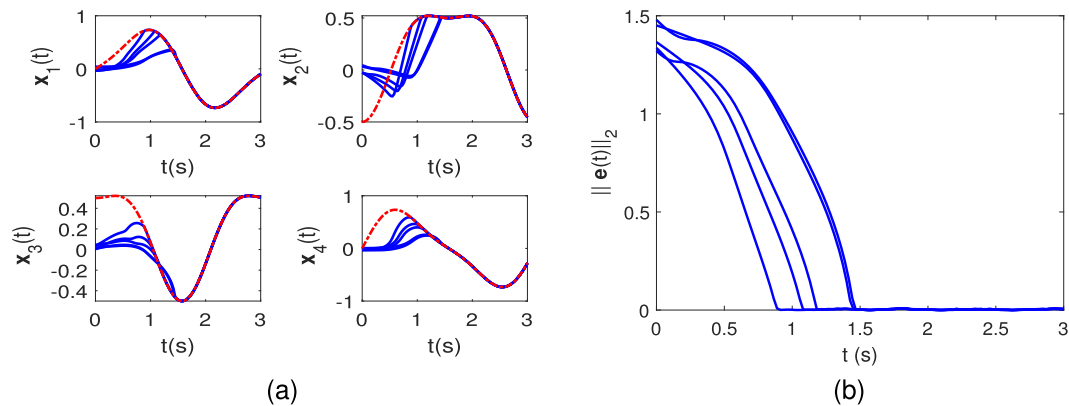


**FIGURE 4.** Simulative results of solving the TVLE problem (19) by the AAGND-2 model (15) with five random initial states. (a) The trajectories of elements of solution  $x(t)$ , where the blue-solid curves denote the computing solution and the red-dotted curve denotes the theoretical solution. (b) The trajectories of residual error  $\|e(t)\|_2$ .

correctness of Theorem 2 and 3. Specifically, the convergence time of the AAGND-1 (14) model ranges from 0.84 s to 1.37 s, while the convergence time of the AAGND-2 (15) model ranges from 0.89 s to 1.48 s.

**B. APPLICATIONS**

In this part, two applications of AAGND models are demonstrated. One is an application on controlling a robotic manipulator, the other is acoustic location.



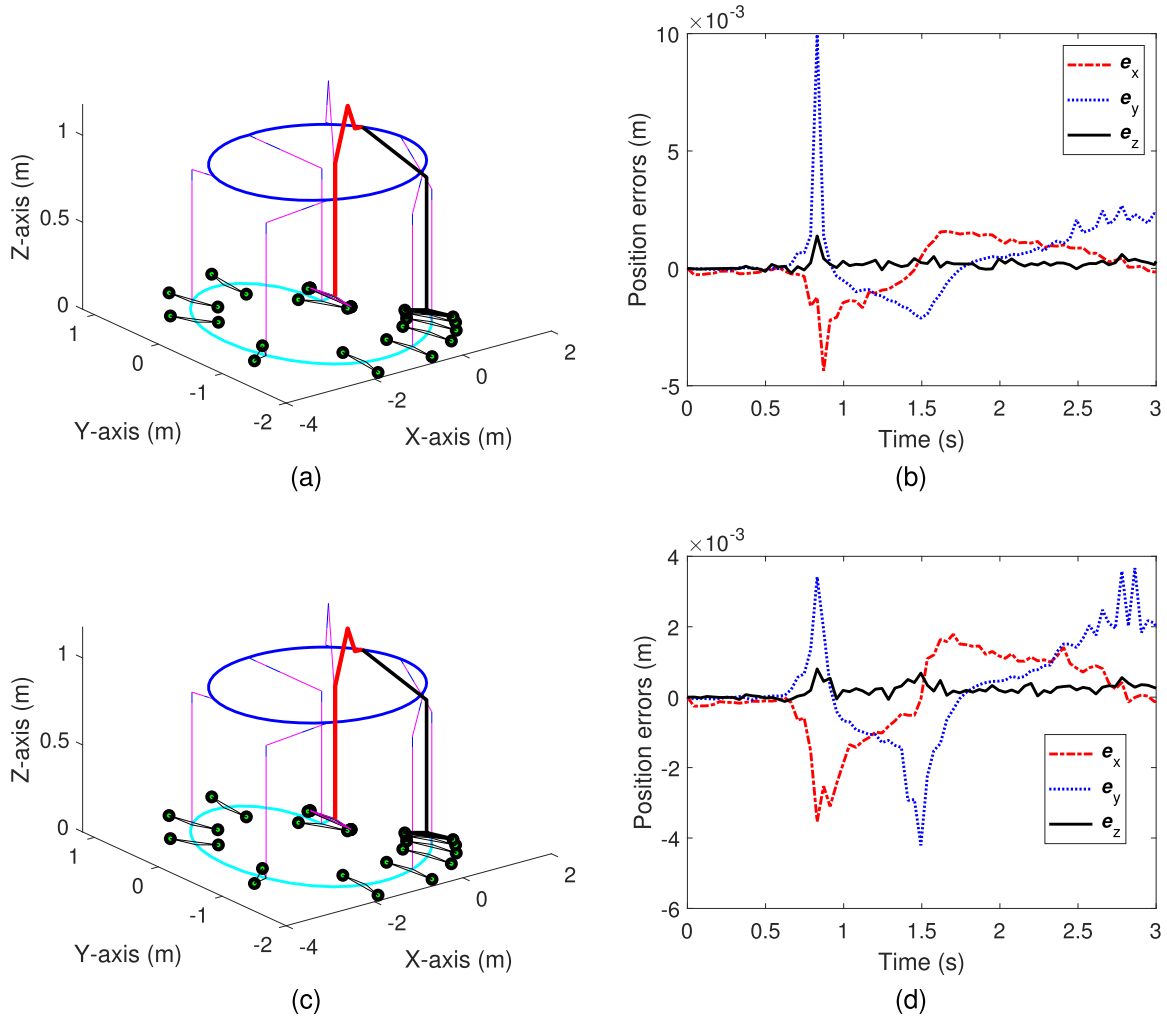


**FIGURE 5.** Results of application on robot control. (a) Demonstration of movements of the whole wheeled mobile manipulator synthesized by the AAGND-1 model (22). (b) Position error of the end-effector synthesized by the AAGND-1 model (22). (c) Demonstration of movements of the whole wheeled mobile manipulator synthesized by the AAGND-2 model (24). (d) Position error of the end-effector synthesized by the AAGND-2 model (24).

1) APPLICATION ON ROBOT CONTROL

In the application on robot control, a mobile robotic manipulator is required to generate a circular path. Generally, the typical model of a kinematic model can be expressed as

$$r(t) = f(\theta(t)), \tag{20}$$

in which  $r(t)$  is the position vector of the end-effort of the manipulator,  $f(\cdot)$  is a smooth nonlinear projected function, and  $\theta(t)$  represents a vector combining the angle of the mobile platform and the joint-space of the manipulator [29]. Then, an error function can be constructed as

$$e_1(t) = r(t) - f(\theta(t)). \tag{21}$$

Following the derivation of AAGND models, the corresponding AAGND-1 model in this application is

$$\dot{\theta}(t) = -\exp(\|e_1(t)\|_2)\sigma_1(t)\left(\frac{\partial f(\theta(t))}{\partial \theta(t)}\right)^T e_1(t). \tag{22}$$

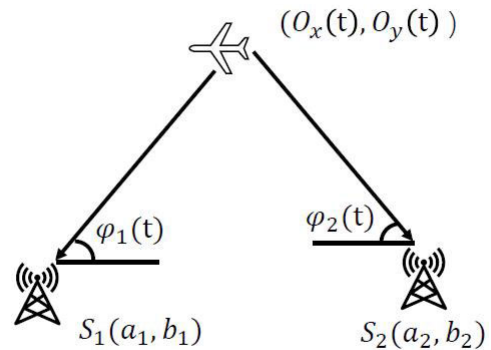


**FIGURE 6.** The diagram of the AOA technology for acoustic location.

where

$$\sigma_1(t) = \alpha \frac{\|e_1^T(t)\dot{r}(t)\|}{\|e_1^T(t)\frac{\partial f(\theta(t))}{\partial \theta(t)}\|_2^2}. \tag{23}$$

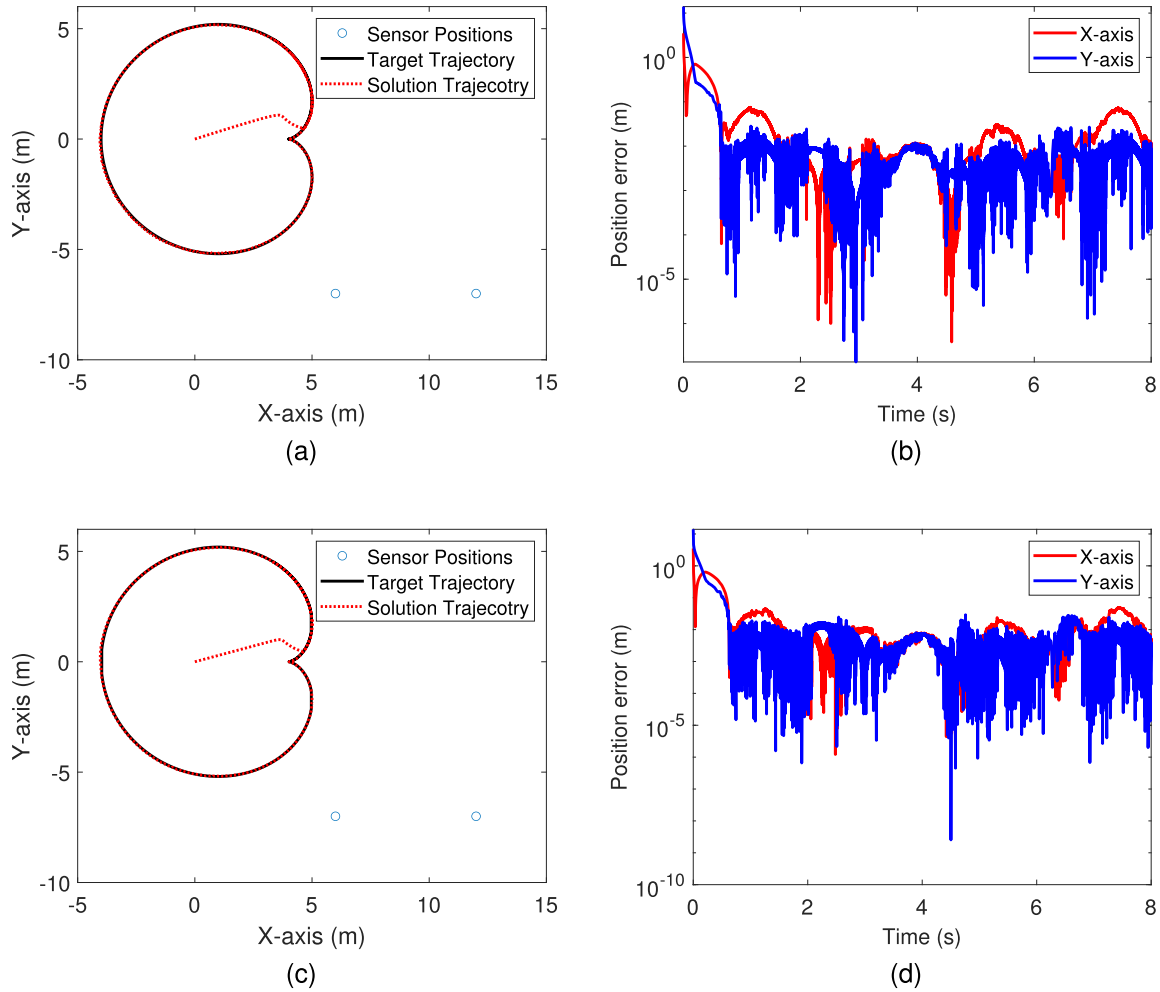


**FIGURE 7.** Results of application on acoustic location. (a) Demonstration of the trajectory generated by the AAGND-1 model (14). (b) Absolute values of the position errors in the X-axis and Y-axis generated by the AAGND-1 model (14). (c) Demonstration of the trajectory generated by the AAGND-2 model (15). (d) Absolute values of the position errors in the X-axis and Y-axis generated by the AAGND-2 model (15).

Similarly, the AAGND-2 model in this application can be expressed as

$$\dot{\theta}(t) = -\sigma_1(t) \left( \frac{\partial f(\theta(t))}{\partial \theta(t)} \right)^T \Gamma(e_1(t)). \quad (24)$$

With  $\alpha = 2$  and the initial state  $\theta(0) = [0, 0, \frac{\pi}{12}, \frac{\pi}{3}, \frac{\pi}{3}, \frac{\pi}{3}, \frac{\pi}{3}, \frac{\pi}{3}]$ , experimental results are shown in Fig. 5, where the first row illustrates the results of the AAGND-1 model (22) and the second row illustrates results of the AAGND-2 model (24). According to Fig. 5(a) and (c), both the end-efforts controlled by the AAGND-1 model (22) and the AAGND-2 model (24) can generate the circle path. Moreover, their position errors are shown in Fig. 5(b) and (d), respectively. The maximum position of the AAGND-1 model (22) is about 10<sup>-3</sup> m, while the one of the AAGND-2 model (24) is about 4<sup>-3</sup> m. Consequently, the proposed AAGND models are efficient in the application on robot control.

## 2) APPLICATION ON ACOUSTIC LOCATION

Among prevalent technologies of acoustic location, many models of these technologies are formulated as time-variant linear equations that could be solved by the AAGND models [9], [30], [31]. For brevity and simplification, a demonstration of the two-dimension arrival of angle (AOA) acoustic location is provided, whose diagram is shown in Fig. 6. As indicated in Fig. 6, a simple moving object located at  $(O_x(t), O_y(t))$  reflects the acoustic wave to two sensors  $S_1$  and  $S_2$  with arrival angles  $\varphi_1(t)$  and  $\varphi_2(t)$ , respectively. Moreover, the location of  $S_1$  is  $(a_1, b_1)$ , while the one of  $S_2$  is  $(a_2, b_2)$ . Therefore, according to the geometry of the AOA model, we have

$$\begin{aligned} \tan(\varphi_1(t)) &= \frac{O_y(t) - b_1}{O_x(t) - a_1}, \\ \tan(\varphi_2(t)) &= \frac{O_y(t) - b_2}{O_x(t) - a_2}. \end{aligned} \quad (25)$$

After reconstruction, (25) can be transformed into a linear equation as

$$\begin{bmatrix} -\tan(\varphi_1(t)) & 1 \\ -\tan(\varphi_2(t)) & 1 \end{bmatrix} \times \begin{bmatrix} O_x(t) \\ O_y(t) \end{bmatrix} = \begin{bmatrix} b_1 - a_1 \tan(\varphi_1(t)) \\ b_2 - a_2 \tan(\varphi_2(t)) \end{bmatrix}, \quad (26)$$

which is a special case of (3). Therefore, AAGND models can be exploited in AOA acoustic location.

With  $\alpha = 2$  and initial solution (0, 0), the results of this application are shown in Fig. 7. In Fig. 7(a) and (c), blue circles denote the sensors, black-solid curve denotes the real trajectory of the moving object, and the red-dotted curve denotes the estimated trajectory synthesized by the proposed model. As indicated in these figures, the estimated trajectory of the moving object well traces the real trajectory, illustrating the efficiency of AAGND models. Moreover, the profiles of the absolute value of position error in the X-axis and Y-axis are shown in Fig. 7(c) and (d), where the position errors are at the level of  $10^{-2}$  m. Over all, the proposed AAGND models can successfully solve the acoustic location problem.

## V. CONCLUSION

This paper revisits the limitations among prevalent models for solving the TVLE and presents AAGND models for improvement. With an adaptive parameter, the AAGND model can eliminate not only the theoretical error but also the matrix inverse. Moreover, by inserting a time-variant coefficient or employing an activation function, AAGND models have a faster convergence rate. These superior properties have been theoretically proven and experimentally validated. Furthermore, applications on robot control and acoustic location utilizing AAGND models are demonstrated, where AAGND models can successfully complete these tasks. In the future, we will look for further improvement in the accuracy and convergence rate of the proposed models. Besides this, more practical application scenarios should be investigated.

## DECLARATION OF COMPETING INTEREST

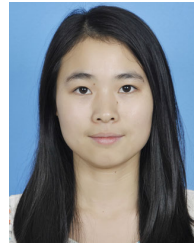
The authors declare that they have no known competing financial interests or personal relationships that could have appeared to influence the work reported in this paper.

## REFERENCES

- [1] K. Kumar Sharma, D. Gurjar, M. Jyotyana, and V. Kumari, "Denosing of brain MRI images using a hybrid filter method of Sylvester-Lyapunov equation and non local means," in *Smart Innovations in Communication and Computational Sciences*. Singapore: Springer, 2019, pp. 495–505.
- [2] A. Purkayastha, "Lyapunov equation in open quantum systems and non-hermitian physics," *Phys. Rev. A, Gen. Phys.*, vol. 105, no. 6, Jun. 2022, Art. no. 062204.
- [3] G. Wang, Z. Hao, B. Zhang, and L. Jin, "Convergence and robustness of bounded recurrent neural networks for solving dynamic Lyapunov equations," *Inf. Sci.*, vol. 588, pp. 106–123, Apr. 2022.
- [4] S. Yuan, M. Lv, S. Baldi, and L. Zhang, "Lyapunov-equation-based stability analysis for switched linear systems and its application to switched adaptive control," *IEEE Trans. Autom. Control*, vol. 66, no. 5, pp. 2250–2256, May 2021.
- [5] P. Axelsson and F. Gustafsson, "Discrete-time solutions to the continuous-time differential Lyapunov equation with applications to Kalman filtering," *IEEE Trans. Autom. Control*, vol. 60, no. 3, pp. 632–643, Mar. 2015.
- [6] A. Perrusquía and W. Yu, "Identification and optimal control of nonlinear systems using recurrent neural networks and reinforcement learning: An overview," *Neurocomputing*, vol. 438, pp. 145–154, May 2021.
- [7] A. N. Win and M. Li, "Numerical method based on fiber bundle for solving Lyapunov matrix equation," *Math. Comput. Simul.*, vol. 193, pp. 556–566, Mar. 2022.
- [8] G. Wang, H. Huang, L. Shi, C. Wang, D. Fu, L. Jin, and X. Xiuchun, "A noise-suppressing Newton-raphson iteration algorithm for solving the time-varying Lyapunov equation and robotic tracking problems," *Inf. Sci.*, vol. 550, pp. 239–251, Mar. 2021.
- [9] X. Xiao, C. Jiang, Q. Mei, and Y. Zhang, "Noise-tolerate and adaptive coefficient zeroing neural network for solving dynamic matrix square root," *CAAI Trans. Intell. Technol.*, early access, doi: 10.1049/cit2.12183.
- [10] C. Jiang and X. Xiao, "Norm-based adaptive coefficient ZNN for solving the time-dependent algebraic Riccati equation," *IEEE/CAA J. Automatica Sinica*, vol. 10, no. 1, pp. 298–300, Jan. 2023.
- [11] Y. Liu, K. Liu, G. Wang, Z. Sun, and L. Jin, "Noise-tolerant zeroing neurodynamic algorithm for upper limb motion intention-based human-robot interaction control in non-ideal conditions," *Expert Syst. Appl.*, vol. 213, Mar. 2023, Art. no. 118891.
- [12] L. Jia, L. Xiao, J. Dai, Z. Qi, Z. Zhang, and Y. Zhang, "Design and application of an adaptive fuzzy control strategy to zeroing neural network for solving time-variant qp problem," *IEEE Trans. Fuzzy Syst.*, vol. 29, no. 6, pp. 1544–1555, Jun. 2021.
- [13] M. Zheng, C. Jiang, Y. Liufu, and X. Xiao, "A non-convex activation and noise-suppressing zeroing neural network for finding time-varying matrix square root," *IEEE Access*, vol. 10, pp. 128336–128347, 2022.
- [14] G. Wang, Q. Li, S. Liu, H. Xiao, and B. Zhang, "New zeroing neural network with finite-time convergence for dynamic complex-value linear equation and its applications," *Chaos, Solitons Fractals*, vol. 164, Nov. 2022, Art. no. 112674.
- [15] Z. Sun, G. Wang, L. Jin, C. Cheng, B. Zhang, and J. Yu, "Noise-suppressing zeroing neural network for online solving time-varying matrix square roots problems: A control-theoretic approach," *Expert Syst. Appl.*, vol. 192, Apr. 2022, Art. no. 116272.
- [16] Y. He, L. Xiao, F. Sun, and Y. Wang, "A variable-parameter ZNN with predefined-time convergence for dynamic complex-valued Lyapunov equation and its application to AOA positioning," *Appl. Soft Comput.*, vol. 130, Nov. 2022, Art. no. 109703.
- [17] L. Xiao and Y. Zhang, "Zhang neural network versus gradient neural network for solving time-varying linear inequalities," *IEEE Trans. Neural Netw.*, vol. 22, no. 10, pp. 1676–1684, Oct. 2011.
- [18] G. Wang, Z. Hao, H. Li, and B. Zhang, "An activated variable parameter gradient-based neural network for time-variant constrained quadratic programming and its applications," *CAAI Trans. Intell. Technol.*, early access, doi: 10.1049/cit2.12192.
- [19] L. Jin, L. Wei, and S. Li, "Gradient-based differential neural-solution to time-dependent nonlinear optimization," *IEEE Trans. Autom. Control*, vol. 68, no. 1, pp. 620–627, Jan. 2023.
- [20] L. Lv, J. Chen, L. Zhang, and F. Zhang, "Gradient-based neural networks for solving periodic Sylvester matrix equations," *J. Franklin Inst.*, vol. 359, no. 18, pp. 10849–10866, Dec. 2022.
- [21] G. Sowmya, P. Thangavel, and V. Shankar, "A novel hybrid Zhang neural network model for time-varying matrix inversion," *Eng. Sci. Technol., Int. J.*, vol. 26, Feb. 2022, Art. no. 101009.
- [22] Z. Fu, Y. Zhang, and N. Tan, "Gradient-feedback ZNN for unconstrained time-variant convex optimization and robot manipulator application," *IEEE Trans. Ind. Informat.*, early access, Jan. 31, 2023, doi: 10.1109/TII.2023.3240737.
- [23] J. Yan, X. Xiao, H. Li, J. Zhang, J. Yan, and M. Liu, "Noise-tolerant zeroing neural network for solving non-stationary Lyapunov equation," *IEEE Access*, vol. 7, pp. 41517–41524, 2019.
- [24] L. Xiao and B. Liao, "A convergence-accelerated Zhang neural network and its solution application to Lyapunov equation," *Neurocomputing*, vol. 193, pp. 213–218, Jun. 2016.
- [25] V. N. Katsikis, P. S. Stanimirovic, S. D. Mourtas, L. Xiao, D. Karabasevic, and D. Stanujkic, "Zeroing neural network with fuzzy parameter for computing pseudoinverse of arbitrary matrix," *IEEE Trans. Fuzzy Syst.*, vol. 30, no. 9, pp. 3426–3435, Sep. 2022.
- [26] L. Jin, S. Li, B. Liao, and Z. Zhang, "Zeroing neural networks: A survey," *Neurocomputing*, vol. 267, pp. 597–604, Dec. 2017.
- [27] G. H. Golub and C. F. Van Loan, *Matrix Computations*. Johns Hopkins Univ. Press, 2013.



- [28] B. Datta, *Numerical Methods for Linear Control Systems*, vol. 1. New York, NY, USA: Academic, 2004.
- [29] X. Yan, M. Liu, L. Jin, S. Li, B. Hu, X. Zhang, and Z. Huang, "New zeroing neural network models for solving nonstationary Sylvester equation with verifications on mobile manipulators," *IEEE Trans. Ind. Informat.*, vol. 15, no. 9, pp. 5011–5022, Sep. 2019.
- [30] G. Wang, Z. Hao, B. Zhang, L. Fang, and D. Mao, "A robust Newton iterative algorithm for acoustic location based on solving linear matrix equations in the presence of various noises," *Int. J. Speech Technol.*, vol. 53, no. 2, pp. 1219–1232, Jan. 2023.
- [31] L. Jin, J. Yan, X. Du, X. Xiao, and D. Fu, "RNN for solving time-variant generalized Sylvester equation with applications to robots and acoustic source localization," *IEEE Trans. Ind. Informat.*, vol. 16, no. 10, pp. 6359–6369, Oct. 2020.



**LILAN ZOU** received the M.S. degree from Sun Yat-sen University, China, in 2015. She is currently pursuing the Ph.D. degree with Hainan University, China. She is currently a Lecturer with the College of Electronics and Information Engineering, Guangdong Ocean University. Her recent research interests include nonvolatile electronic devices and their applications in neuromorphic computing and information processing.



**QINROU LI** is currently pursuing the bachelor's degree with the School of Electronic and Information Engineering, Guangdong Ocean University, Zhanjiang, China. Her research interests include sea temperature prediction and neural networks.



**YUYUAN ZHUANG** is currently pursuing the B.S. degree in data science and big data technology with Guangdong Ocean University, Guangdong, China. His research interests include computer vision and neural networks.



**GUANCHENG WANG** received the B.E. degree in automation from Sun Yat-sen University, Guangzhou, in 2014, and the M.S. degree in electrical and computer engineering from the University of Macau, Macau, SAR, China, in 2017. He is an Academic Staff with the School of Electronics and Information Engineering, Guangdong Ocean University, Zhanjiang, China. He has published dozens of articles. His current research interests include neural networks, optimization, and robot control. He served as a Reviewer in several journals, such as *Information Science*, *Applied Soft Computing*, and *CAAI Transactions on Intelligence Technology*.

• • •